Available online at www.sciencedirect.com
SCIENCE DIRECT®
Journal of Solid State Chemistry 178 (2005) 412–418
JOURNAL OF SOLID STATE CHEMISTRY
www.elsevier.com/locate/jssc

Optical spectra of trivalent lanthanides in $LiYF_4$ crystal

K. Ogasawara[a,*], S. Watanabe[a], H. Toyoshima[a], T. Ishii[a], M.G. Brik[b], H. Ikeno[c], I. Tanaka[c]

[a]Department of Chemistry, School of Science and Technology, Kwansei Gakuin University, 2-1 Gakuen, Sanda, Hyogo 669-1337, Japan
[b]Fukui Institute for Fundamental Chemistry, Kyoto University, 34-4, Takano-Nishihiraki-cho, Sakyo-ku, Kyoto 606-8103, Japan
[c]Department of Materials Science and Engineering, Kyoto University, Sakyo, Kyoto 606-8501, Japan

Received 7 May 2004; received in revised form 31 October 2004; accepted 1 November 2004

Abstract

Systematic calculations of multiplet energy levels of all trivalent lanthanides in $LiYF_4$ (YLF) crystal were performed using two completely different approaches: diagonalization of the commonly used semi-empirical Hamiltonian and a fully relativistic discrete-variational multi-electron (DV-ME) method which is based on a first-principles configuration-interaction (CI) calculation program using molecular spinors obtained by the discrete-variational Dirac–Slater (DV-DS) calculations. The energy level diagrams within $4f^n$ electron configurations were obtained by the former method, while those including both $4f^n$ and $4f^{n-1}5d^1$ configurations were obtained by the latter. Using the explicit many-electron wave functions, the absorption spectra of Pr^{3+}, Ho^{3+}, and Tm^{3+} in YLF were calculated and compared with the experimental data.

Keywords: Trivalent lanthanides; Multiplets; Energy levels; Dieke diagram; First-principles calculation; Configuration interaction

1. Introduction

The $4f^n$ energy levels of trivalent lanthanides (Ln^{3+}) in $LaCl_3$ up to 40,000 cm^{-1} have been reported in details by Dieke's group almost four decades ago [1]. Their energy level diagram is widely known as "Dieke diagram" [2] and regarded as a general reference of the energy levels of trivalent lanthanides. Later Carnall et al. [3,4] have performed detailed calculations of the $4f^n$ energy levels of trivalent lanthanides in different environments based on the commonly used semi-empirical Hamiltonian and extended the Dieke diagram up to 50,000 cm^{-1}. Recently, higher energy levels of trivalent lanthanides in $LiYF_4$ (YLF) have been explored by Meijerink et al. [5,6] by measuring excitation spectra using synchrotrons and the Dieke diagram has been extended up to almost 70,000 cm^{-1}. Since the technological importance of higher energy levels is rapidly growing due to the strong demand for luminescent materials or solid-state lasers in the ultraviolet (UV) or vacuum ultraviolet (VUV) regions, the extension of the Dieke diagram toward the higher energy region is becoming more and more important. These energy regions generally correspond to the high-lying $4f^n$ and $4f^{n-1}5d^1$ configurations.

In order to investigate energy levels higher than 70,000 cm^{-1}, we have recently performed theoretical calculations of free trivalent lanthanides based on two different approaches [7]: one is a calculation based on the commonly used semi-empirical Hamiltonian and the other is a fully relativistic discrete-variational multi-electron (DV-ME) method which is based on a first-principles configuration-interaction (CI) calculation program using molecular spinors obtained by the

*Corresponding author. Fax: +81 79 565 7943.
E-mail address: ogasawara@ksc.kwansei.ac.jp (K. Ogasawara).

0022-4596/$ - see front matter © 2004 Elsevier Inc. All rights reserved.
doi:10.1016/j.jssc.2004.11.001

discrete-variational Dirac–Slater (DV-DS) calculations [8]. The complete energy levels of $4f^n$ configurations were calculated using the former while complete energy levels of both $4f^n$ and $4f^{n-1}5d^1$ configurations were calculated using the latter. In the case of the relativistic DV-ME method, calculated energy levels are overestimated typically by 20–30%. However, if we introduce a certain element-specific scaling factor (0.7–0.8) [7], the results of the DV-ME method agrees quantitatively with those of the semi-empirical method. The large overestimation of multiplet energy is probably due to the underestimation of electron correlations since only the Ln-4*f* and Ln-5*d* orbitals are considered in these CI calculations.

The crystal-field calculations of $4f^n$–$4f^{n-1}5d^1$ absorption spectra of Ln^{3+} in YLF have been performed by Reid et al. and Pieterson et al. and the general features of the experimental excitation spectra have been reproduced by estimating appropriate sets of parameters [9,10]. However, the energy levels of $4f^{n-1}5d^1$ configurations significantly depend on the host crystal due to the strong covalency between the Ln 5*d* orbitals and the ligand orbitals. Therefore, the crystal-field parameters for $4f^{n-1}5d^1$ configurations should also be significantly dependent on the host crystal. Accordingly, the determination of appropriate parameter sets generally requires a lot of experience and expertise in this field.

On the other hand, a first-principles calculation can be performed for any ions in an arbitrary environment without introduction of any empirical parameters, i.e., without requiring any preliminary experience. Therefore, investigation of the energy levels and optical spectra using a first-principles method is expected to give some basic information for appropriate semi-empirical analysis of materials whose electronic structures are completely unknown.

In this paper, we have performed systematic calculations of energy levels of trivalent lanthanides in YLF as we have done for free trivalent lanthanides in our previous work [7]. Complete energy levels for $4f^n$ configurations were calculated using the semi-empirical method while complete energy levels for $4f^n$ and $4f^{n-1}5d^1$ configurations were calculated using the first-principles relativistic DV-ME method. Using the explicit many-electron wave functions, the absorption spectra of Pr^{3+}, Ho^{3+}, and Tm^{3+} in YLF were also calculated and compared with the experimental data.

2. Computational procedure

The most frequently used form of the semi-empirical Hamiltonian for the calculation of lanthanide ions in crystals is as follows:

$$\begin{aligned} H = H_0 &+ \sum_{k=0,2,4,6} F^k(nf,nf) f_k + \zeta_f A_{SO} \\ &+ \alpha L(L+1) + \beta G(G_2) + \gamma G(R_7) \\ &+ \sum_{i=2,3,4,6,7,8} t_i T^i + \sum_{h=0,2,4} m_h M^h \\ &+ \sum_{f=2,4,6} p_f P^f + H_{CF}, \end{aligned} \tag{1}$$

where all terms have their usual meaning [4]. Effects of crystal field (if an ion is embedded into a crystal or glass) give rise to the last term in Eq. (1), whose structure is as follows:

$$\begin{aligned} H_{CF} = &\sum_{k=2,4,6} \sum_{m=1}^{N} B_0^k C_0^k(m) \\ &+ \sum_{k=2,4,6} \sum_{q=1}^{k} \sum_{m=1}^{N} [B_q^k (C_q^k(m) \\ &+ (-1)^q C_{-q}^k(k)) \\ &+ B_{-q}^k i (C_{-q}^k(m) - (-1)^q C_q^k(m))]. \end{aligned} \tag{2}$$

B_q^k stand for the crystal-field parameters, and $C_q^k(m)$ are one-electron spherical operators. Matrix elements of all operators entering Eqs. (1) and (2) can be taken from Refs. [11,12]. If the local symmetry of an impurity center is S_4 (as it is the case of the YLF crystal), only the following crystal-field parameters are not equal to zero: $B_0^2, B_0^4, B_4^4, B_0^6, B_4^6$ [13]. For the determination of their numerical values we used the "smoothed crystal-field parameters" approach described in Refs. [14,15]. As reference data, we take the results of the crystal-field analysis for Nd^{3+} and Er^{3+} ions in YLF, which had been performed in Refs. [16,17], respectively. The smoothed crystal-field parameters for the whole series of trivalent lanthanides in the YLF crystal are shown in Table 1. These parameters have been used to get complete energy level schemes for all trivalent lanthanides (except Gd^{3+}) in the YLF crystal.

The fully relativistic DV-ME method is based on a CI calculation program using the four-component fully relativistic molecular spinors obtained by the DV-DS cluster calculations [18]. In this work only those electrons occupying the molecular spinors mainly composed of Ln-4*f* states (impurity ion states) in the ground state were treated explicitly. The relativistic many-electron Hamiltonian used in the calculations can be expressed (in atomic units) as

$$\begin{aligned} H = &\sum_{i=1}^{n} \left[c\alpha \mathbf{p}_i + \beta c^2 - \sum_v \frac{Z_v}{|\mathbf{r}_i - \mathbf{R}_v|} + V_0(\mathbf{r}_i) + \sum_\mu \frac{Z_\mu^{\text{eff}}}{|\mathbf{r}_i - \mathbf{R}_\mu|} \right] \\ &+ \sum_{i=1}^{n} \sum_{j>i}^{n} \frac{1}{|\mathbf{r}_i - \mathbf{r}_j|}, \end{aligned} \tag{3}$$

Table 1

Ion	B_{20}	B_{40}	B_{60}	B_{44}	B_{64}
Ce^{3+}	371	−1103	61	−1657	−1536
Pr^{3+}	354	−946	49	−1421	−1230
Nd^{3+} [16]	379	−957	44	−1206	−1078
Pm^{3+}	338	−781	37	−1174	−933
Sm^{3+}	336	−739	34	−1110	−867
Eu^{3+}	336	−708	33	−1063	−820
Gd^{3+}	336	−681	31	−1024	−779
Tb^{3+}	337	−730	29	−1097	−737
Dy^{3+}	339	−635	28	−955	−696
Ho^{3+}	341	−617	26	−927	−664
Er^{3+} [17]	308	−523	23	−953	−623
Tm^{3+}	347	−593	25	−891	−633
Yb^{3+}	350	−576	24	−866	−598

where n is the number of the Ln-4f electrons in the ground state, $\boldsymbol{\alpha}$, β the Dirac matrices, c the velocity of light, $\mathbf{r}_i$, $\mathbf{p}_i$ the position and the momentum operator of the ith electron, Z_ν and $\mathbf{R}_\nu$ the charge and position of the νth nucleus, Z_μ^{eff} and $\mathbf{R}_\nu$ the effective charge and position of the μth ion outside the model cluster. The electron–electron repulsion term in Eq. (3) denotes the interactions among these explicitly treated electrons. On the other hand, $V_0(\mathbf{r}_i)$ in Eq. (3) denotes the Coulomb potential on these explicitly treated electrons from the other (core and valence) electrons and has the form [19]

$$V_0 = \int \frac{\rho_0^{\mathrm{G}}(\mathbf{r}')}{|\mathbf{r}-\mathbf{r}'|}\,\mathrm{d}\mathbf{r}' + \frac{3}{4}\left[\frac{\rho^{\mathrm{G}}(\mathbf{r})V_{xc}\{\rho^{\mathrm{G}}(\mathbf{r})\} - \rho_0^{\mathrm{G}}(\mathbf{r})V_{xc}\{\rho_0^{\mathrm{G}}(\mathbf{r})\}}{\rho_{\mathrm{imp}}^{\mathrm{G}}(\mathbf{r})} - V_{xc}\{\rho_{\mathrm{imp}}^{\mathrm{G}}(\mathbf{r})\}\right], \quad (4)$$

where ρ^{G}, $\rho_{\mathrm{imp}}^{\mathrm{G}}$, ρ_0^{G} represent the charge density of all electrons, that of the electrons occupying the impurity ion states and that of the remaining (core and valence) electrons, respectively, and V_{xc} is the Slater's $X\alpha$potential. The superscript G indicates the values in the ground state. We have diagonalized the above Hamiltonian within the subspace spanned by the Slater determinants composed of relativistic spinors with dominant Ln-4f or Ln-5d characters and obtained the energy level schemes of $4f^n$ and $4f^{n-1}5d^1$ configurations for all trivalent lanthanides. The diagonalization was performed separately for the states with each irreducible representation.

In the DV-ME calculations, the effect of the host crystal can be directly taken into account by use of model clusters. In principle, it is possible to optimize the geometry around the impurity ions by the total energy minimization using some of the modern quantum chemistry programs. However, in the DV-DS method, Coulomb potentials are calculated in the self-consistent-charge (SCC) approximation [8], where they are spherically averaged around each atom. Although the SCC approximation is advantageous for larger and faster calculations, it makes an accurate calculation of the absolute total energy difficult. Therefore, in this work we constructed a model cluster based on the experimental crystal structure of YLF [20]. An $(LnF_8)^{5-}$ cluster was used for the calculation and the effective Madelung potential was taken into account by locating several thousand point charges at atomic sites outside the cluster. There are several papers [21,22], in which the embedding effects are treated explicitly, by means of introduction of the corresponding terms into the crystal Hamiltonian. This approach allows one to obtain a more precise picture of what is going on in the considered cluster and the crystal and perform the geometry optimization. Since in the present work we focus our attention on the *relative* energy intervals and *relative* intensities in the absorption spectra, the geometry optimization and embedding effects other than the Madelung potential are beyond our consideration and have not been taken into account.

3. Results and discussions

The parameters of the semi-empirical free ion Hamiltonian for all trivalent lanthanides were taken from [4]; they have been used to find the eigenvalues and eigenstates of all trivalent lanthanide ions in a free state. The crystal-field parameters are taken from Table 1. The calculated energy levels of trivalent lanthanides in YLF are given in Fig. 1, where the energy levels for free ions are also shown together for comparison. (The energy levels of Gd^{3+} in YLF have not been obtained yet due to our computational limitation.)

The results of the relativistic CI calculations are also shown in Fig. 2, where the energy levels of $4f^n$ and $4f^{n-1}5d^1$ configurations are shown in the left and right columns. In Fig. 2, the lengths of the lines denote the contribution of each configuration. A short line on the left column indicates a partial contribution of the $4f^n$ configuration and there should be a corresponding short line representing a remaining partial contribution of the $4f^{n-1}5d^1$ configuration to the state on the right column. Although the short lines on the right column are buried in a band formed with the full-length lines, we can estimate their contribution from the composition of $4f^n$ configuration. One can note from Fig. 2 that, in the case of ions in YLF, there exists a significant mixture between $4f^n$ and $4f^{n-1}5d^1$ configurations, which is absent in the case of free ions due to the difference of parity. The origin of this mixture is the lack of gerade/ungerade representations due to the absence of center of symmetry in S_4 point group. The calculated energy levels

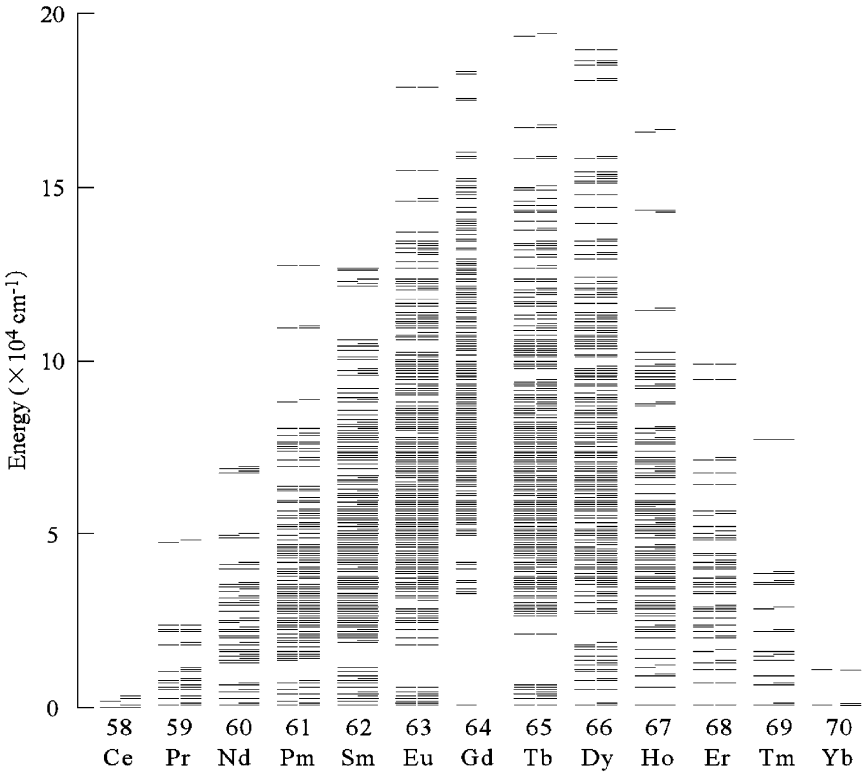

Fig. 1.

are overestimated typically by 20–30%. The major reason for this discrepancy is probably underestimation of electron correlations since only the states mainly composed of Ln-4*f* or Ln-5*d* characters were considered in the CI calculations due to our computational limitations. The inclusion of the other orbitals such as the states mainly composed of F-2*p* character is expected to reduce this overestimation.

Although the energy levels are overestimated in the first-principles method, if we take into account the element-specific scaling factor estimated from the free ion calculations [7], the results of the first-principles method agree well with those of the semi-empirical method and also with the experimental data such as the Dieke diagram. In our work, despite the overestimation of the calculated energy levels, the *relative* energy level intervals are reproduced fairly well, which gives an opportunity of the first-principles prediction of the absorption spectra.

In the DV-ME method, the many-electron wave functions corresponding to each state can be obtained explicitly as linear combinations of the Slater determinants. Therefore, we can calculate the oscillator strengths of the electric dipole transitions directly. Though we obtained the absorption spectra for the whole lanthanide series, we restrict here the presented results to the cases of Pr^{3+}, Ho^{3+}, and Tm^{3+} ions only, to avoid making the paper too lengthy and the theoretical and experimental spectra too small for reading and understanding.

The theoretical absorption spectrum of Pr^{3+} in YLF is compared with the experimental absorption spectrum ($LiLuF_4$:Pr^{3+}) [23] and the experimental excitation spectrum [9] in Fig. 3. For easy comparison with the experimental spectra, each level is broadened with 0.3 eV full-width at half-maximum (FWHM) Gaussian functions. The corresponding multiplet energy levels belonging to each irreducible representation are shown above the spectrum. The *f–d* transition energy is overestimated by about 2.7 eV in this case. This is probably due to the overestimation of the energy interval between $4f^2$ and $4f^15d^1$ configurations. In the experimental spectrum, there are three broad lines labeled as A, B, and C in the figure. The intensities of these peaks gradually increase in the experimental spectra. These features are also reproduced by the ordinary crystal-field calculation [9]. In the present work, the intensity of peak B is relatively overestimated. However, overall features of the spectrum are well-reproduced without any empirical parameters.

The theoretical absorption spectrum of Ho^{3+} in YLF is compared with the experimental excitation spectrum [24] in Fig. 4. Each level is also broadened with 0.1 eV FWHM Gaussian functions. Although the *f–d* transition energy is underestimated by about 0.5 eV, the agreement of the transition energy is better than the case of Pr^{3+}.

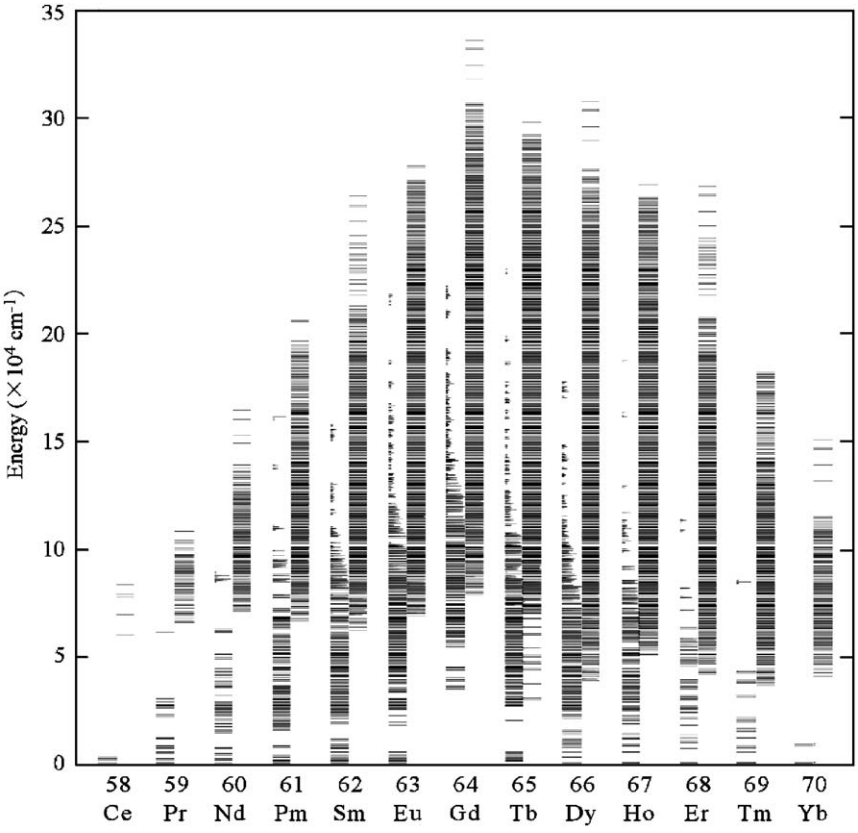

Fig. 2.

This is probably due to the cancellation of the overestimation of the energy intervals between the $4f^{10}$ and $4f^{9}5d^{1}$ configurations and the overestimation of the multiplet splitting of the $4f^{9}5d^{1}$ configuration. The former would increase the f–d transition energies while the latter would decrease the threshold energy of the f–d transitions. In the experimental spectrum, there are mainly five broad lines labeled as A, B, C, D, and E in the figure. There are characteristic features among the intensities of these peaks: the intensity changes alternately until peak D, and peak E is the strongest. These features are also reproduced by the CF calculation [10]. According to the first-principles calculations shown in Fig. 5, the number of energy levels of this configuration is quite large and they almost form a band. However, when the transition probabilities from the ground state to these levels are calculated, only a limited number of states contribute to the peaks in the spectrum. As a result, the characteristic features of the experimental spectrum were well-reproduced by the nonempirical relativistic CI calculation.

The theoretical absorption spectrum of Tm^{3+} in YLF is compared with the experimental excitation spectrum [24] in Fig. 5. Each level is also broadened with 0.1 eV FWHM Gaussian functions. The f–d transition energy is underestimated by about 2.5 eV in this case. Again, this is probably due to the competition between the overestimation of the energy intervals between the $4f^{12}$ and $4f^{11}5d^{1}$ configurations and the overestimation of the multiplet splitting of the $4f^{11}5d^{1}$ configuration. In this case, the latter is dominant due to the larger number of $4f$ electrons. In the experimental spectrum, there are mainly five broad lines labeled as A, B, C, D, and E in the figure. The intensities of these peaks gradually decrease except the last one (peak E). In the theoretical spectra the intensities of peak A are underestimated, the reason of which is currently unknown. Even in the CF calculation reported by Pieterson et al. [10], there is similar underestimation of the intensity of peak A. Therefore, the intensity variation is difficult to reproduce even by the CF calculation. One of the possible reasons of this discrepancy is the effect of broadening. In this work, we have broadened each peak uniformly. However, the peak widths can be different for each peak. The number of energy levels of this configuration is also quite large in this case. However, when the transition probabilities from the ground state to these levels are calculated, only a limited number of states contribute to the peaks in the spectrum and the relative peak positions were well-reproduced by the nonempirical relativistic CI calculation.

The wave functions of the $4f^{n-1}5d^{1}$ configurations are expected to strongly depend on the interactions with the

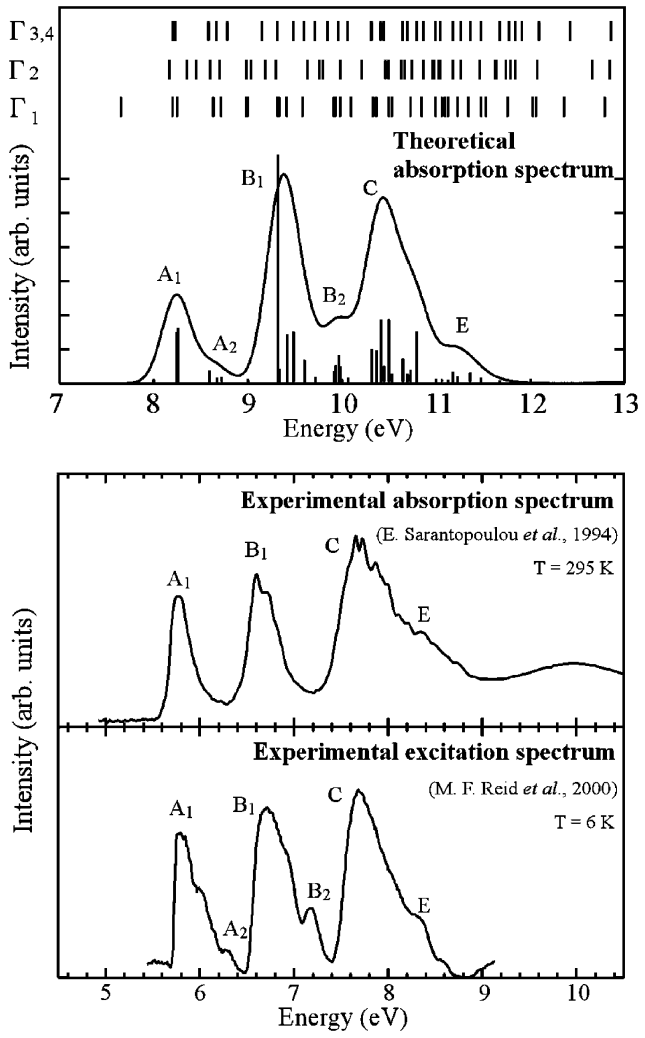

Fig. 3.

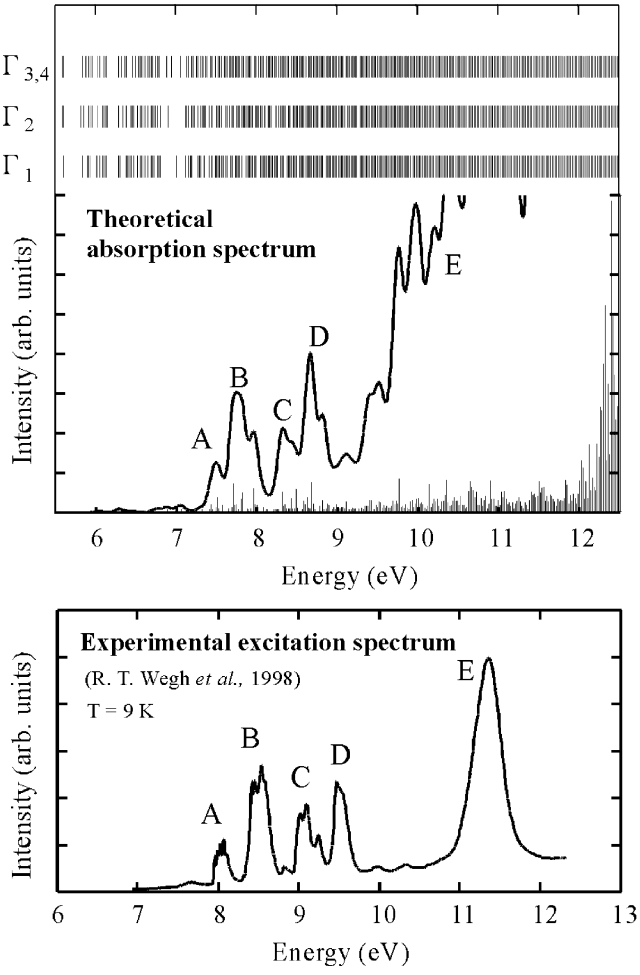

Fig. 4.

host crystal. Therefore, the reasonable agreement between the theoretical spectrum and experimental spectra demonstrated for three ions indicates that the calculated many-electron wave functions include these effects and can be used for the prediction of basic features of *f–d* transition spectra. Calculations of the absorption spectra for all other lanthanides embedded in YLF and comparison with experimental data will be reported elsewhere [25].

4. Conclusions

In the present work, systematic energy level calculations for all trivalent lanthanides in YLF have been performed for $4f^n$ and $4f^{n-1}5d^1$ electronic configurations using two completely different approaches. The complete $4f^n$ energy levels were obtained by semi-empirical calculations and the complete $4f^n$ and $4f^{n-1}5d^1$ energy levels were obtained by the fully relativistic DV-ME method. The results of the two approaches are in good agreement with each other if a certain element-specific scaling factor was taken into account for the DV-ME results. In the case of trivalent lanthanides in YLF, the mixture between the $4f^n$ and $4f^{n-1}5d^1$ electronic configurations, which is due to the absence of inversion symmetry originating from the interactions between the lanthanides and the host crystal, was estimated quantitatively. The absorption spectra of Pr^{3+}, Ho^{3+}, and Tm^{3+} in YLF were calculated using the explicitly obtained many-electron wave functions. Though the absolute positions of the energy levels are not reproduced exactly, the relative separations between the energy levels and the shape of the absorption spectra are reproduced fairly well without any empirical parameters. The discrepancy in the absolute energy is probably due to the underestimation of electron correlations and is expected to be improved by extending the basis for CI calculations (e.g., inclusion of states with F-2*p* or Ln-6*s*, 6*p*, etc.). The geometry optimization around the lanthanide ions as well as the consideration of embedding effects beyond the simple Madelung potential may also improve the results [21,22].

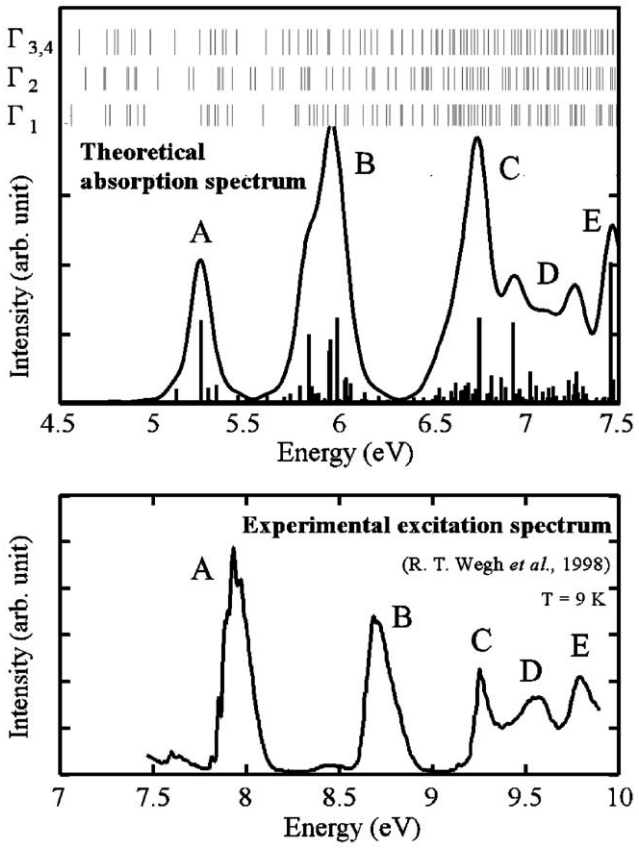

Fig. 5.

Acknowledgements

K. Ogasawara was supported in part by the Industrial Technology Research Grant Program in '01 from the New Energy and Industrial Technology Development Organization (NEDO) of Japan, and in part by a Grant-in-Aid for Scientific Research from the Japanese Ministry of Education, Culture, Sports, Science and Technology (MEXT). M.G. Brik is financially supported by the Japanese Ministry of Education, Culture, Sports, Science and Technology (MEXT) in a project on computational materials science unit at Kyoto University.

Note added in proof

Detailed review of the trends in crystal field parameters for trivalent lanthanides in $LiYF_4$ based on the thorough analysis of experimental results available in the literature [26, and references therein] has been published few weeks after this paper had been accepted for publication.

References

[1] G.H. Dieke, H.M. Crosswhite, Appl. Opt. 2 (7) (1963) 675.
[2] G.H. Dieke, Spectra Energy Levels of Rare Earth Ions in Crystals, Wiley Interscience, New York, 1968.
[3] W.T. Carnall, P.R. Fields, K. Rajnak, J. Chem. Phys. 49 (1968) 4424.
[4] W.T. Carnall, G.L. Goodman, K. Rajnak, R.S. Rana, J. Chem. Phys. 90 (1989) 3443.
[5] A. Meijerink, R.T. Wegh, Mater. Sci. Forum 315–317 (1999) 11.
[6] R.T. Wegh, A. Meijerink, R.-J. Lamminmäki, J. Hölsä, J. Lumin. 87–89 (2000) 1002.
[7] K. Ogasawara, S. Watanabe, Y. Sakai, H. Toyoshima, T. Ishii, M.G. Brik, I. Tanaka, Jpn. J. Appl. Phys. 43 (2004) L611.
[8] J. Onoe, H. Nakamatsu, T. Mukoyama, R. Sekine, H. Adachi, K. Takeuchi, Inorg. Chem. 36 (1997) 1934.
[9] M.F. Reid, L. van Pieterson, R.T. Wegh, A. Meijerink, Phys. Rev. B 62 (2000) 14744.
[10] L. van Pieterson, M.F. Reid, R.T. Wegh, S. Soverna, A. Meijerink, Phys. Rev. B 65 (2000) 045114.
[11] C.W. Nielsen, G.F. Koster, Spectroscopic Coefficients for the p^n, d^n, and f^n Configurations, The MIT Press, Cambridge, MA, 1963.
[12] Argonne National Laboratory's web site (Hannah Crosswhite's data files): http://chemistry.anl.gov/downloads/index.html
[13] D.J. Newman, B. Ng (Eds.), Crystal Field Handbook, Cambridge University Press, Cambridge, 2000.
[14] C.A. Morrison, R.P. Leavitt, J. Chem. Phys. 71 (6) (1979) 2366.
[15] C.A. Morrison, R.P. Leavitt, J. Chem. Phys. 74 (1) (1981) 25.
[16] E. Rukmini, C.K. Jayasankar, M.F. Reid, J. Phys.: Condens. Matter 6 (1994) 5919.
[17] R.T. Wegh, E.V.D. van Loef, G.W. Burdick, A. Mejerink, Mol. Phys. 101 (7) (2003) 1047.
[18] K. Ogasawara, T. Iwata, Y. Koyama, T. Ishii, I. Tanaka, H. Adachi, Phys. Rev. B 64 (2001) 115413.
[19] S. Watanabe, H. Kamimura, Mater. Sci. Eng. B 3 (1989) 313.
[20] A.V. Goryunov, A.I. Popov, Russ. J. Inorg. Chem. 37 (1992) 126.
[21] R. Llusar, M. Casarrubios, Z. Barandiaran, L. Seijo, J. Chem. Phys. 105 (1996) 5321.
[22] L. Seijo, Z. Barandiaran, J. Chem. Phys. 118 (2003) 5335.
[23] E. Sarantopoulou, C. Cefalas, A.M. Dubinskii, A.C. Nicolaides, Y.R. Abdulsabirov, L.S. Korableva, K.A. Naumov, V.V. Semashko, Appl. Phys. Lett. 15 (1994) 813.
[24] R.T. Wegh, H. Donker, A. Meijerink, Electrochem. Soc. Proc. 97–29 (1998) 284.
[25] K. Ogasawara, S. Watanabe, H. Toyoshima, T. Ishii, M.G. Brik, H. Ikeno, I. Tanaka, in preparation.
[26] C. Rudowicz, J. Qin, J. Alloys Compd. 385 (2004) 238.